

# A Comparison between the Stress-Relaxation Behavior of Molybdenum and Polyethylene

B. HAGSTRÖM,\* J. KUBÁT, and M. RIGDAHL,† *Chalmers University of Technology, Department of Polymeric Materials, S-412 96 Gothenburg, Sweden*

## Synopsis

The stress-relaxation behaviors of molybdenum (Mo) and polyethylene are compared, especially with regard to the role played by the internal stress level, in the relation  $F = 0.1(\sigma_0 - \sigma_i)$ . Here  $F$  is the maximum slope in the inflexion region of stress vs.  $\ln$  time curves ( $\sigma$  vs.  $\ln t$ ),  $\sigma_0$  is the initial stress, and  $\sigma_i$  is the internal (equilibrium) stress. Despite a significant difference in  $\sigma_i$  in the two materials, this relation was obeyed in both cases. The data for Mo are for room temperature and 90 K; those for low and high density polyethylene for room temperature only. Some of the data are reevaluated results of earlier measurements. The shape of the  $\sigma_i(\epsilon)$  curves is reminiscent of the  $\sigma(\epsilon)$  behavior for both Mo and polyethylene. The implications of the results for interpretation of the relaxation process in terms of current theoretical concepts is discussed.

## INTRODUCTION

The flow behavior of metals and polymers (creep, stress-relaxation) is often described in terms of different theoretical concepts. For metals the theory of stress-aided thermal activation (SDTA) or a power law approach is commonly employed,<sup>1-3</sup> while for polymers the flow is usually interpreted using the idea of a relaxation time spectrum (RTS).<sup>4,5</sup> Despite the difference in the analytical tools used, the relaxation (and creep) behavior of metals and polymers exhibits many fundamental similarities. Particularly significant in this connection is a relation between the maximum slope of the stress-relaxation curve of almost any solid, irrespective of its structure, and the initial stress  $\sigma_0$ <sup>6,7</sup>:

$$F = \left( - \frac{d\sigma}{d \ln t} \right)_{\max} = 0.1(\sigma_0 - \sigma_i) \quad (1)$$

where  $\sigma$  denotes the time-dependent stress,  $t$  the time, and  $\sigma_i$  the internal stress, i.e., the equilibrium stress level approached after sufficiently long times. Equation (1) is valid in temperature regions where no structural changes in the material occur; the scatter of the numerical constant 0.1 is about 10%.<sup>6</sup> There are also counterparts to eq. (1) relating to the creep behavior of materials (see, e.g., Ref. 8).

\*Present address: Neste Polyeten AB, Box 44, S-444 01 Stenungsund, Sweden.

†Also with: Swedish Pulp and Paper Research Institute, Paper Technology Department, Box 5604, S-114 86 Stockholm, Sweden.

Equation (1) shows that the internal stress is an important parameter with a significant influence on the shape of the relaxation curve.<sup>3,7</sup>

The present paper analyzes experimental results obtained in relaxation experiments with drawn, polycrystalline molybdenum wire. The behavior of Mo is compared to that of low and high density polyethylene (LDPE, HDPE) studied earlier.<sup>9,10</sup> A central point in this evaluation is eq. (1), which is found to be obeyed by both Mo and PE. Special interest is devoted to the behavior at large deformations (above yield).

The basic idea behind comparing Mo with PE is a significant difference in the internal stress level. In the light of the definition of the effective stress, entering eq. (1) as  $(\sigma_0 - \sigma_i)$ , choosing Mo and PE for this comparison thus appears to provide a useful platform for a further assessment of the validity of this equation. Some of the Mo data presented below are reevaluated results of measurements on Mo at RT and 90 K.<sup>11</sup>

### THEORETICAL BACKGROUND

Before reporting on the experimental results, we give a brief outline of the basic theoretical concepts used to describe the stress-relaxation behavior of solids. For polymers, this process is usually interpreted in terms of the RTS concept,<sup>4,5</sup> giving  $\sigma(t)$  as

$$\sigma(t) = \epsilon_0 \int_{-\infty}^{\infty} H(\tau) e^{-t/\tau} d \ln \tau + \sigma_i \quad (2)$$

Here  $\epsilon_0$  is the initially applied constant strain,  $H(\tau)$  the distribution of relaxation times  $\tau$ , and  $\sigma_i$  the internal stress. This approach is formal only and gives no insight into the flow mechanism behind the  $H(\tau)$  function.

For metals and other crystalline solids, the SDTA theory is the commonly used tool. The basic equation is as follows<sup>2</sup>:

$$\dot{\sigma} = \frac{d\sigma}{dt} = -A \exp[v(\sigma - \sigma_i)/kT] \quad (3)$$

where  $A$  is a constant (preexponential) factor,  $v$  the activation volume,  $k$  Boltzmann's constant, and  $T$  the absolute temperature. The difference between the actual applied stress  $\sigma$  and the internal stress  $\sigma_i$  is often called the effective stress,  $\sigma^*$ .

Equation (3) corresponds approximately to a straight line in a  $\sigma(\log t)$  diagram. It is often found to be valid at shorter relaxation times (higher stresses), while at longer times a deviation from eq. (3) is observed. This latter region of the relaxation curve can often be described by a power law relation<sup>2</sup>

$$\dot{\sigma} = -B(\sigma - \sigma_i)^n \quad (4)$$

where  $B$  and  $n$  are constants, their values depending on the nature of the material and the temperature. The transition from the exponential law behavior (SDTA) to a power law dependence occurs at a certain critical stress,  $\sigma_{tr}$ , given by<sup>9</sup>

$$(\sigma_{tr} - \sigma_i)/(\sigma_0 - \sigma_i) = n/10 \quad (5)$$

Neither of the theoretical approaches [eqs. (2)–(4)] can, however, be reconciled with the experimentally well-documented numerical constant of eq. (1). Recently a cooperative model has been suggested that accounts for the constant 0.1 in eq. (1).<sup>12,13</sup> This theory is based on a two-level model, where flow units are raised to an upper energy level during the initial straining of the solid. During the return to the lower level, phonons are emitted which stimulate transitions of unrelaxed flow units. In this way, multiple transitions of varying size may occur, producing in a natural fashion a distribution of relaxation times. The relaxation process is described by

$$(\kappa/\tau)\sigma^* = \beta[\psi(\beta + \beta t/\tau) - \psi(1 + \beta t/\tau)] \quad (6)$$

where  $\kappa$  is a constant,  $\tau$  is a relaxation time,  $\psi(x)$  the digamma function, and  $\beta = (-6\kappa\dot{\sigma}_0^*/\pi^2)^{1/2}$ . The parameter  $\beta$  is related to the maximum slope of  $F$  in eq. (1) as

$$F = (\ln \beta + \gamma)^{-1}(\sigma_0 - \sigma_i) \quad (7)$$

where  $\gamma$  is Euler's constant (0.5778...). The constant 0.1 in eq. (1) corresponds to  $\log(-\kappa\dot{\sigma}_0^*) \approx 8.4$ . It has also been shown that there is an upper limit ( $s_m$ ) to the size of the multiple transitions, and that this explains the value of the constant of proportionality in eq. (1).<sup>13</sup> The cooperative model may formally be transformed into a discrete relaxation time distribution  $H(\tau)$  given by (cf. Ref. 14)

$$\begin{aligned} H(\tau_s) &= \frac{1}{e^{s/\beta} - 1} && \text{for } \tau/s_m \leq \tau_s \leq \tau \\ &= 0 && \text{otherwise} \end{aligned} \quad (8)$$

with the relaxation times given by

$$\tau, \tau/2, \tau/3, \dots, \tau/s_m \quad (9)$$

and  $s$  being an integer varying from 1 to  $s_m$ . The cooperative model may thus be said to have a spectral character.

It should be mentioned that the cooperative model describes the exponential law region (SDTA region) of the relaxation curve but not, at this stage, the power law region. The ability of eq. (6) to describe the experimental relaxation behavior of a wide range of materials is demonstrated in Ref. 15.

## EXPERIMENTAL

### Materials

The molybdenum wire used in this work was 99.95% pure. It was produced by hot drawing to a diameter of 0.4 mm, producing a highly oriented grain structure. Wide angle X-ray diffraction revealed that the fiber axis was [110]. The grain diameter of the longitudinal section was ca. 2–3  $\mu\text{m}$ . No further treatment of the wires was performed prior to the relaxation experiments.

### Methods

The stress relaxometer used has been described earlier.<sup>16</sup> The measurements were carried out at  $25 \pm 0.1^\circ\text{C}$  and the initial strain rate was  $8 \times 10^{-3} \text{ s}^{-1}$ . Some experiments with a lower strain rate ( $6.7 \times 10^{-5} \text{ s}^{-1}$ ) were also performed. The effective gauge length of the wires was 80 mm. The maximum deformation ( $\epsilon_0$ ) was about 0.7%. The combined elastic stiffness of the Mo wire and the relaxometer amounted to 270 GPa. Thus the relaxometer can be regarded as sufficiently stiff. The additional strain induced during the relaxation process was accordingly small in comparison with the initially applied strain  $\epsilon_0$ .

## RESULTS AND COMMENTS

### Stress-Strain Behavior

Figure 1 shows the stress-strain curves of the Mo wires at room temperature. The strain rate was  $8 \times 10^{-3} \text{ s}^{-1}$ . The curves are rather linear up to a strain level of ca. 0.15% (corresponding stress ca. 350–400 MPa). The relaxation experiments were performed in both the linear and the nonlinear regions.

### The Shape and the Position of the Stress-Relaxation Curves

Figure 2 shows examples of stress-relaxation curves given as  $\sigma/\sigma_0$  vs.  $\log t$ , for the Mo wires at three different initial deformations  $\epsilon_0$ : 0.15, 0.26, and 0.57%. An increase in  $\epsilon_0$  shifts the relaxation curves towards shorter times; this shift may be interpreted in terms of a strain dependence of the constants  $A$  or  $B$  of eqs. (3) and (4). It is, however, not linked to a cutoff of the relaxation time spectrum due to a longer initial straining time since this normally produces a shift in the opposite direction. Figure 2 also includes relaxation data for high density polyethylene (HDPE) obtained at large deformations.<sup>10</sup> With HDPE a shift to shorter times of the relaxation curves with increasing values of  $\epsilon_0$  is observed; with low density polyethylene (LDPE) the shift is towards longer times.<sup>10</sup>

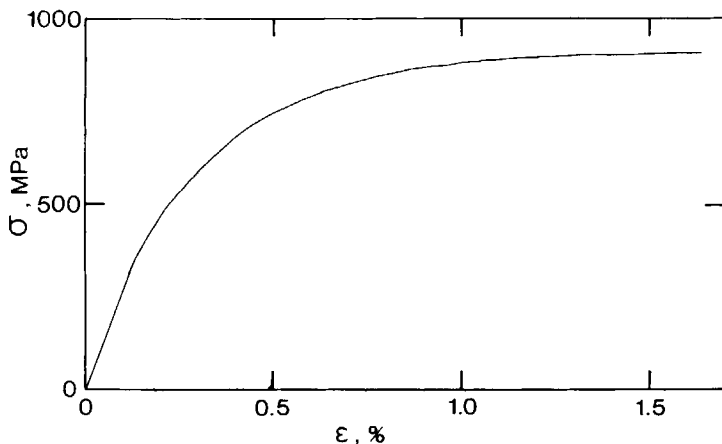


Fig. 1. Stress-strain curves at  $25^\circ\text{C}$  for the Mo-wire, strain rate was  $8 \times 10^{-3} \text{ s}^{-1}$ .

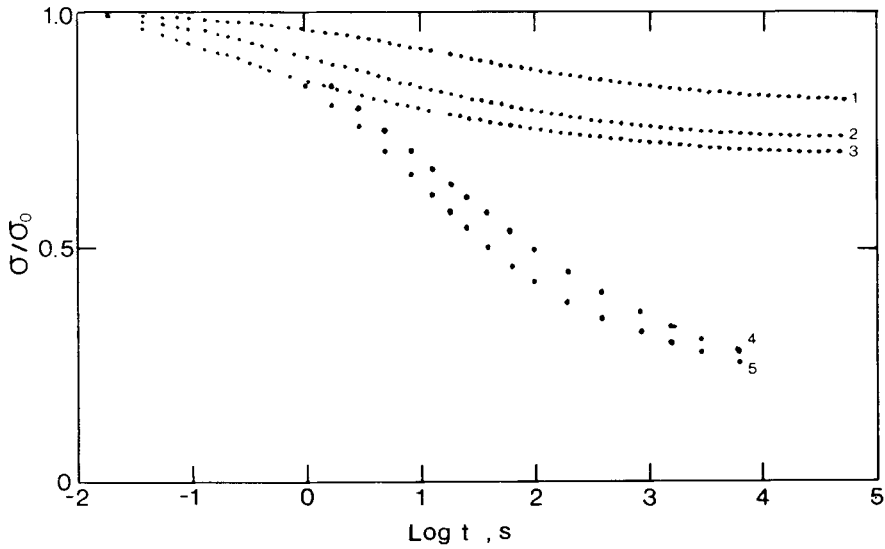


Fig. 2. Stress-relaxation curves for (·) Mo and (●) HDPE<sup>10</sup> at room temperature given as  $\sigma/\sigma_0(\log t)$ . Key for initial elongation (%): (1) 0.15; (2) 0.36; (3) 0.57; (4) 1.5; (5) 9.6.

With regard to the relaxable stress there is a striking difference between the behavior of Mo and HDPE. As can be seen in Figure 2, this stress appears to be substantially smaller for Mo than for HDPE, i.e., the stress approaches asymptotically higher values of  $\sigma/\sigma_0$  at longer times for Mo than for HDPE (and for LDPE). This is due to a difference in the internal stress level,  $\sigma_i$ . The influence of  $\sigma_i$  on the shape of the relaxation curves can be eliminated by plotting the curves as  $(\sigma - \sigma_i)/(\sigma_0 - \sigma_i)$  vs.  $\log t$ . (The determination of  $\sigma_i$  is

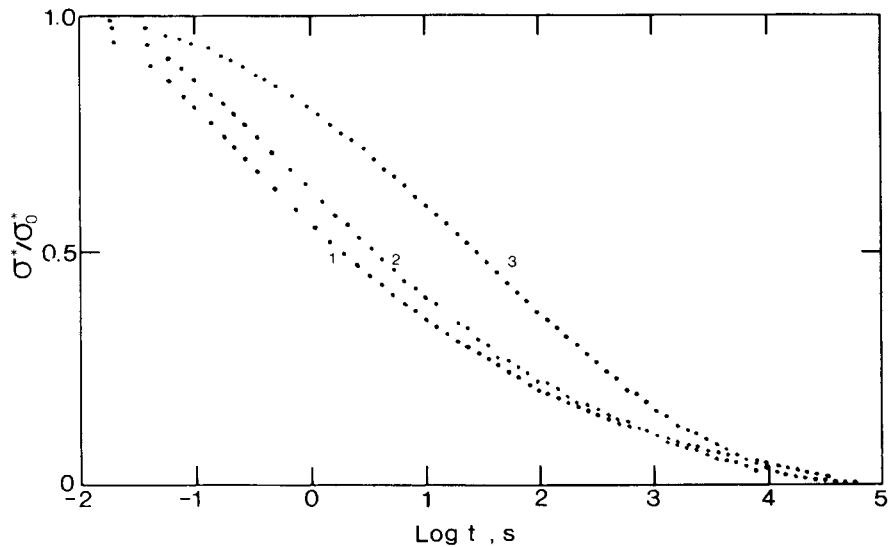


Fig. 3. Stress-relaxation curves for Mo given as  $\sigma^*/\sigma_0^*$  vs.  $\log t$ . Key for initial elongation (%): (1) 0.51; (2) 0.26; (3) 0.10.

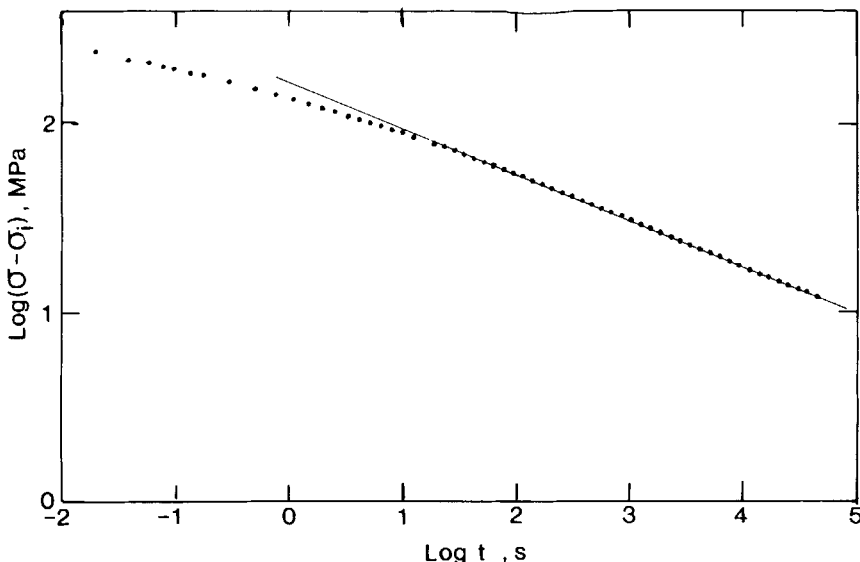


Fig. 4.  $\log(\sigma - \sigma_i)$  vs.  $\log t$  for Mo at 25°C. Initial deformation 0.43%.

discussed in a following section.) This is shown in Figure 3, and, as can be seen, the curves are approximately linear at higher values of  $\sigma^*/\sigma_0^*$  (shorter times). In this region the curves can be described by the SDTA theory or the cooperative model, eq. (6). Again, there is a shift of the curves towards shorter times with increasing  $\epsilon_0$ .

At longer times the relaxation curves are better described by the power law, eq. (4). This is shown in Figure 4, where  $\log(\sigma - \sigma_i)$  is shown as a function of  $\log t$ . The curves are linear at longer times in agreement with eq. (4). The values of the exponent  $n$  in the power law is ca. 7 irrespective of the applied strain  $\epsilon_0$ . The corresponding values for HDPE and LDPE are 5–6 and 5, respectively.<sup>10</sup> The  $n$  values for Mo are in good agreement with those reported by Gupta and Li,<sup>17</sup> who found a constant value of 7.5 in the strain interval 1–12%. It may also be added that Prekel and Conrad<sup>18</sup> found the value 6.4 for the dislocation velocity–stress exponent for Mo at room temperature.

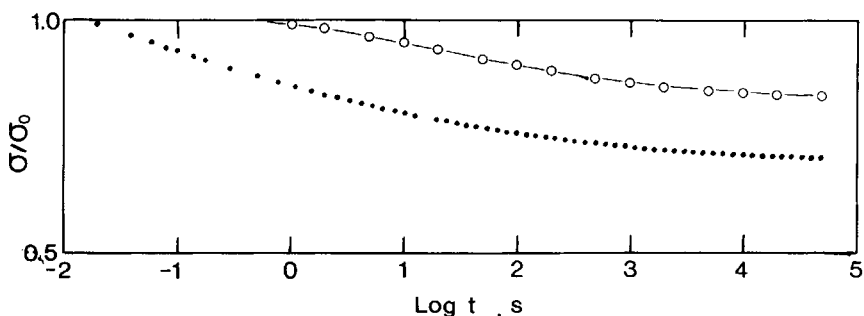


Fig. 5. Stress-relaxation curves for Mo obtained at two different initial strain rates: (●)  $8 \times 10^{-3}$  and (○)  $6.7 \times 10^{-5} \text{ s}^{-1}$ . Initial deformation 0.57% in both cases.

Figure 5 shows the effect of the initial strain rate  $\dot{\epsilon}$  on the position of the relaxation curves along the time axis. A decrease in strain rate from  $8 \times 10^{-3} \text{ s}^{-1}$  to  $6.7 \times 10^{-5} \text{ s}^{-1}$  shifts the curve to longer times. The initial deformation  $\epsilon_0$  was 0.57% in both cases. The apparent shift of the curves to longer times is in agreement with the hypothesis of a cutoff of the initial parts of the relaxation time spectrum  $H(\tau)$ .<sup>19</sup>

### Internal Stresses

In accordance with previous works,<sup>9,10</sup> we have found that the internal stress is identical with the stress level approached in the relaxation experiment at very long times. The  $\sigma_i$  values may be evaluated by the method proposed by Li,<sup>20</sup> based on plotting  $-d\sigma/d \log t$  vs.  $\sigma$  and then extrapolating the curve to zero stress rate. The intersection with the stress axis is taken as the internal stress. Figure 6 shows  $\sigma_i$  as function of  $\epsilon_0$ . The curve is rather similar to the  $\sigma(\epsilon)$  curve for the Mo wire. It is linear below  $\epsilon_0 \approx 0.15\%$  and

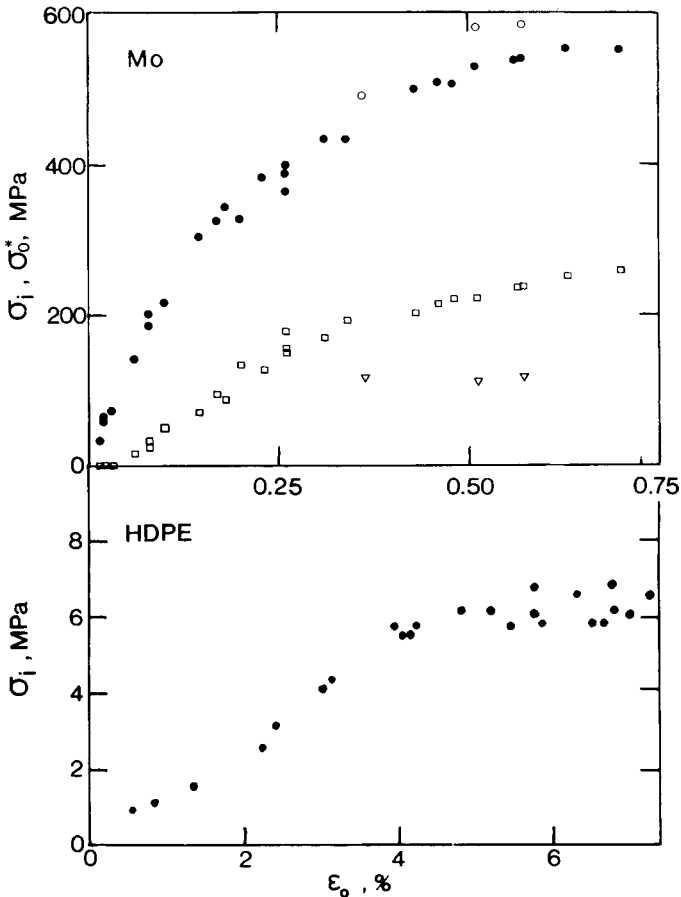


Fig. 6. The (●) internal and (□) effective stress vs. the initial elongation  $\epsilon_0$  for Mo at 25°C. Some data (○ and ▽) have been obtained at a lower initial strain rate ( $6.7 \times 10^{-5} \text{ s}^{-1}$ ). The figure also contains the corresponding data for (●) HDPE.<sup>10</sup> Note the difference in scale between Mo and HDPE.

markedly nonlinear at higher deformations. The  $\sigma_i$  value is thus very closely connected to the deformation  $\epsilon_0$ , and the curve passes through the origin. The  $\sigma_i(\epsilon_0)$  curve for HDPE<sup>10</sup> is also included in Figure 6. Again, there is a similarity between the curves for Mo and HDPE. Note, however, the difference in deformation.

There is, on the other hand, a clear difference between Mo and HDPE in another respect. For Mo,  $\sigma_i$  is significantly higher than the corresponding effective stress  $\sigma^* = \sigma - \sigma_i$  (see Fig. 6). For HDPE and LDPE the reverse is true, the internal stress amounting only to ca. 20% of the applied stress.<sup>10</sup> Thus the viscoelastic character is not very pronounced for Mo compared with polyethylene, at least at room temperature. It should be noted that for  $\epsilon_0$  below ca. 0.1% the effective stress  $\sigma^*$  for Mo is virtually zero. The Mo wire thus does not exhibit any relaxation at low deformations, and the internal stress is thus identical to the initially applied stress  $\sigma_0$ . This may indicate that the term "internal stress" in this context is not very adequate, since it is the stress that the sample can sustain over an extended period of time. This is true for metals as well as polymers.

In Figure 6 a few  $\sigma_i$  values determined using relaxation with a low initial strain rate ( $6.7 \times 10^{-5} \text{ s}^{-1}$ ) are included. The  $\sigma_i$  values are of the same order as those obtained at higher  $\dot{\epsilon}$ , but the  $\sigma^*$  values are significantly lower at the low strain rate (Fig. 6). This is in agreement with the idea that some part of the stress relaxes during a slow straining, i.e., the relaxation spectrum is cut off.

### The Maximum Slope $F$ of the $\sigma(\ln t)$ Curves

Figure 7 shows the maximum slope  $F = (-d\sigma/d \ln t)_{\text{max}}$  of the relaxation curves for Mo vs.  $\sigma_0$  and  $\sigma_0^*$  ( $= \sigma_0 - \sigma_i$ ). The region of the maximum slope coincides with the linear region of the  $\sigma(\log t)$  curves shown in Figure 2. The  $F(\sigma_0)$  curves appear to be composed of two straight segments. The intersection between those straight lines occurs at ca. 350 MPa, which is close to the linearity limit of the stress-strain curve (Fig. 1). The slight change in relaxation behavior is hardly surprising since also the internal stress varies with the applied strain in a nonlinear fashion. A similar change in the  $F(\sigma_0)$  curve has been reported for HDPE<sup>10</sup> and some bcc metals.<sup>21</sup> Again, it should be noted that below ca. 100 MPa, Mo does not relax at all, i.e.,  $F/\sigma_0 = 0$ .

When  $F$  is plotted vs.  $\sigma_0^* = \sigma_0 - \sigma_i$ , a single straight line passing through the origin is obtained (Fig. 7). The slope of this line is 0.105 which is in very good agreement with eq. (1). It should be underlined that a straight line relation is obtained despite the fact that both the linear (elastic) and nonlinear portions of the  $\sigma(\epsilon)$  curve for Mo are contained in this graph.

### Stress-Relaxation of Mo at 90 K

In an earlier work,<sup>11</sup> the stress-relaxation behavior of Mo at 90 K ( $-183^\circ\text{C}$ ) has been reported. It may be interesting to reanalyze these data to obtain more information regarding the internal stresses and their effect on the relaxation behavior. By applying the Li method to the relaxation data given in Ref. 11,  $\sigma_i$  and  $\sigma_0^*$  may be determined as a function of  $\epsilon_0$ . This is shown in Figure 8. The internal stress varies approximately linearly with  $\epsilon_0$  up to ca.



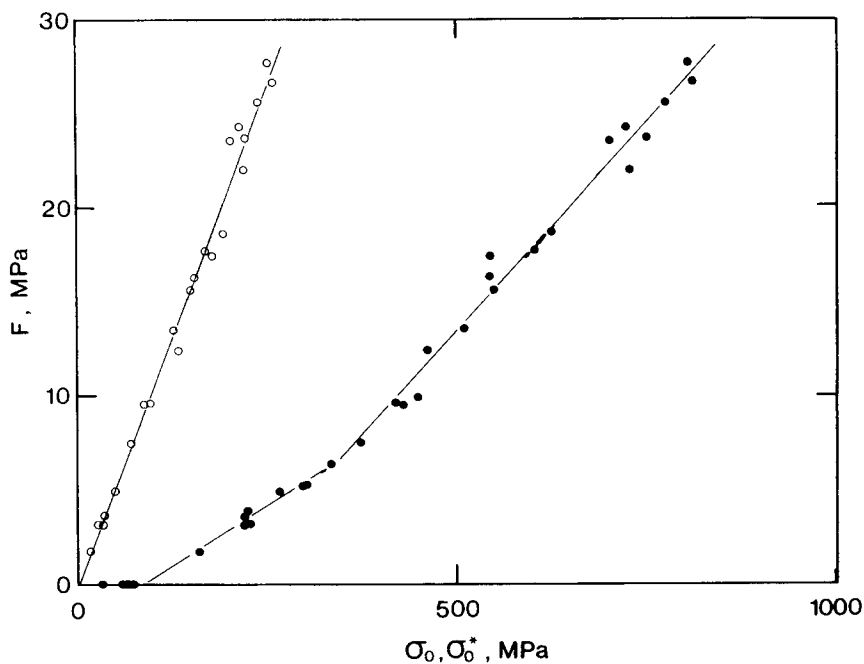


Fig. 7. The maximum slope  $F = (-d\sigma/d \ln t)_{\max}$  vs. (●)  $\sigma_0$  and (○)  $\sigma_0^*$  for Mo at 25°C.

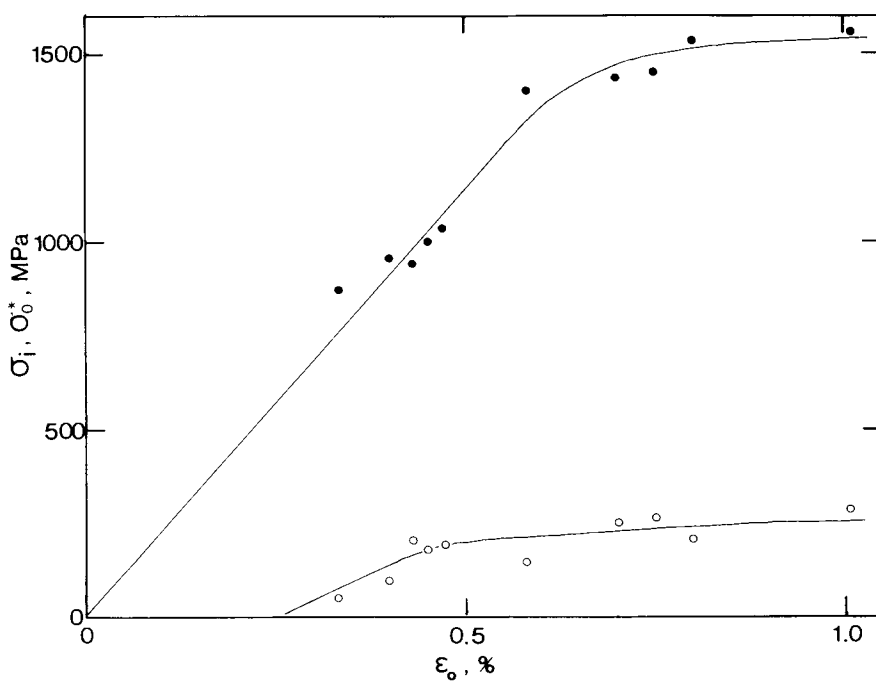


Fig. 8. The (●) internal and (○) effective stress vs.  $\epsilon_0$  for Mo at 90 K ( $-183^\circ\text{C}$ ).

0.6%, which is a parallel to the  $\sigma(\epsilon)$  behavior of Mo at 90 K. The internal stress level is also higher at 90 K than at 298 K (25°C), but the maximum effective stresses are of the same order, ca. 200 MPa. For Mo the relaxable stresses are thus not markedly affected by the temperature, while  $\sigma_i$  varies in a manner related to the  $\sigma(\epsilon)$  properties. For polyethylene, however,  $\sigma_i$  appeared to be rather insensitive to changes in temperature,<sup>9</sup> although the temperature range was significantly smaller in this case (about 45°C).

The data in Figure 8 also show that below approximately 0.25% strain Mo does not relax, i.e.,  $\sigma^* = 0$ , and the specimens behave like elastic solids. Further, it is evident that the relaxation is initiated at lower  $\epsilon_0$  values than those corresponding to the linearity limit of the  $\sigma(\epsilon)$  curves. This can also be seen from the relaxation behavior at 25°C (Fig. 6) and, even more clearly, at low temperatures. Stress-relaxation thus occurs at stress levels below any yield point in the  $\sigma(\epsilon)$  curves (microplasticity).

The  $F/\sigma_0^*$  ratio for Mo at 90 K is 0.098,<sup>11</sup> which is a strong support for the temperature independence of eq. (1).

### FINAL REMARKS

The stress-relaxation behavior of polycrystalline molybdenum appears to fit well into the general pattern given by eq. (1), according to which the slope of the  $\sigma(\log t)$  curves is proportional to  $\sigma_0 - \sigma_i$ . In this case,  $\sigma_i$  constitutes a substantial part of  $\sigma_0$ , in contrast to polymers like polyethylene, where the opposite is true. Despite this difference, eq. (1) is obeyed in both cases as is evident from the data presented above. Although these results are only a small part of the material compiled in order to provide support for eq. (1), they deserve special attention in view of the large variability of  $\sigma_i$  encountered in this case.

Apart from these similarities between Mo and PE, there are also some differences worth mentioning. For instance, the Mo samples exhibit no flow when strained below a critical level (Fig. 7). For PE and other polymers, such a level does not exist, there being always measurable flow also at the lowest stresses.

In both the RTS and the SDTA descriptions as well as in the cooperative model, the use of an internal stress concept is necessary for a correct description of the observed flow behavior. The term "internal" might, however, be superfluous since the corresponding stress simply, in the case of stress-relaxation, is the nonrelaxable stress level, i.e., that part of the initial stress which is stable toward thermal fluctuations on a long-term basis.

As mentioned above, neither the RTS nor the SDTA theory can explain eq. (1). The RTS theory, being a linear approach, complies however with linearity inherent in eq. (1), i.e., the stress rate  $\dot{\sigma}$  varies linearly with a change in  $\sigma_0$ , while the SDTA does not. The cooperative model appears to provide sound physical mechanism for describing the flow process, and it may also provide an explanation to the constant of proportionality in eq. (1). The cooperative model can also be said to be of a spectral character, which means that it complies with the above-mentioned linearity.

The SDTA model, given by eq. (3), cannot explain the experimentally observed linear relation between  $\dot{\sigma}$  and  $\sigma_0$ . Such a linearity can however be

imposed on the SDTA theory by using eq. (1) and the relation<sup>7</sup>

$$F = kT/v \quad (10)$$

The nonlinearity of SDTA, expressed as  $\dot{\sigma}(\sigma)$ , may now, indeed, be apparent only, at least when it comes to the description of relaxation processes which do not shift their position along the  $(\log t)$ -axis when  $\sigma_0$  is changed. If this is the case, the process may be considered linear with regard to  $\sigma_0$ , despite the exponential character of the  $\dot{\sigma}(\sigma)$  relation [eq. (3)]. The source of the rather common misinterpretation of the significance of this equation is the fact that  $\dot{\sigma}(\sigma)$  is supposed to be a unique relation between  $\dot{\sigma}$  and  $\sigma$ , a given stress always producing the same  $\dot{\sigma}$  value. This appears, however, to be untrue. Instead, one has to distinguish the role of  $\sigma$  during a single relaxation process from that of varying  $\sigma_0$ , i.e., the role of  $\sigma$  when several processes at varying  $\sigma_0$  are considered. While  $\dot{\sigma}(\sigma)$  during relaxation at a given  $\sigma_0$  value certainly is exponential, as required by the linearity of  $\sigma$  vs.  $\log t$ , there is nothing to prevent the process from being linear with regard to  $\sigma_0$ . This is also what LVE requires. As a matter of fact, LVE allows any nonlinear  $\dot{\sigma}(\sigma)$  relation during the relaxation to describe the process, since such  $\dot{\sigma}(\sigma)$  relations are nothing more than transformations of the relaxation function of LVE into a  $\dot{\sigma}(\sigma)$  form. Only when the relaxation function is given by  $\exp(-kt)$  is the corresponding  $\dot{\sigma}(\sigma)$  relation linear.

As is well known, such behavior is never observed in practice, all commonly observed relaxation functions giving rise to nonlinear  $\dot{\sigma}(\sigma)$  relations. Although they offer physically plausible explanations to the flow mechanisms in solids when considering the time variation of  $\sigma$  within a single relaxation process, it appears an inadmissible generalization to extend their applicability also to the variation of  $\sigma_0$ . This latter parameter simply seems to produce a linear scale-up of the process in the sense of LVE. There are, of course, numerous instances of a shift of the relaxation curves towards shorter times, implying that  $\sigma_0$  operates in the sense of SDTA, but in the case of low stresses this is generally not true. In Ref. 22 this dependence was resolved by introducing two  $\dot{\sigma}(\sigma)$  exponentials, one of them operating via  $\sigma$  according to eq. (3), the other being the equivalent of the relaxation function in the sense of LVE, scaling linearly with  $\sigma_0$ . The first term takes care of the shift of the relaxation curves along the  $(\log t)$ -axis as  $\sigma_0$  is varied.

The authors thank the Swedish Board for Technical Development for financial support. Thanks are also due to Dr. Ch. Högfors for valuable discussions and to Mrs. K. Thörneby for skilful assistance in the preparation of this manuscript.

### References

1. F. Garofalo, *Fundamentals of Creep and Creep Rupture*, Macmillan, New York, 1965.
2. R. De Batist and A. Callens, *Phys. Stat. Solidi (a)*, **21**, 591 (1974).
3. A. A. Solomon and W. D. Nix, *Acta Metall.*, **18**, 863 (1970).
4. A. Tobolsky, *Properties and Structure of Polymers*, Wiley, New York, 1960.
5. I. M. Ward, *Mechanical Properties of Solid Polymers*, Wiley-Interscience, London, 1971.
6. J. Kubát, *Nature (London)*, **204**, 3781 (1965).
7. J. Kubát and M. Rigdahl, *Mater. Sci. Eng.*, **24**, 223 (1976).
8. L. C. E. Struik, *Physical Aging in Amorphous Polymers and Other Materials*, Elsevier, Amsterdam, 1978.

9. J. Kubát, M. Rigdahl, and R. Seldén, *J. Appl. Polym. Sci.*, **20**, 2799 (1976).
10. J. Kubát, R. Seldén, and M. Rigdahl, *J. Appl. Polym. Sci.*, **22**, 1715 (1978).
11. J. Kubát and C. Pattranie, *Ark. Fys. (Sweden)*, **28**, 365 (1965).
12. C. Högfors, J. Kubát, and M. Rigdahl, *Phys. Stat. Solidi (b)*, **107**, 147 (1981).
13. J. Kubát, *Phys. Stat. Solidi (b)*, **111**, 599 (1982).
14. C. Högfors, J. Kubát, and M. Rigdahl, *Rheol. Acta*, **24**, 250 (1985).
15. J. Kubát, L.-Å. Nilsson, and W. Rychwalski, *Res. Mech.*, **5**, 309 (1982).
16. J. Kubát, *Ark. Fys. (Sweden)*, **25**, 285 (1963).
17. I. Gupta and J. C. M. Li, *Metall. Trans.*, **1**, 2323 (1970).
18. H. L. Prekel and H. Conrad, *Acta Metall.*, **15**, 955 (1967).
19. F. S. Chang, *J. Appl. Polym. Sci.*, **8**, 37 (1964).
20. J. C. M. Li, *Can. J. Phys.*, **45**, 493 (1967).
21. P. Feltham and A. Hawkins, *Mater. Sci. Eng.*, **17**, 239 (1975).
22. J. Kubát, M. Rigdahl, and R. Seldén, *Phys. Stat. Solidi (a)*, **50**, 117 (1978).

Received August 21, 1987

Accepted August 31, 1987